Infrared conductivity and electron–molecular-vibration coupling in the organic superconductor di[bis(ethylenedithio)tetrathiafulvalene] bis(isothiocyanato)cuprate(I), κ-(BEDT-TTF)$_2$ [Cu(NCS)$_2$]: Protonated and deuterated salts

Tadashi Sugano, Hakuro Hayashi, and Minoru Kinoshita
The Institute for Solid State Physics, The University of Tokyo, Roppongi, Minato-ku, Tokyo 106, Japan

Koichi Nishikida
Perkin-Elmer Japan, Kitasaiwai, Nishi-ku, Yokohama 220, Japan
(Received 23 December 1988)

Polarized reflectance spectra of the organic superconductors protonated and deuterated κ-(BEDT-TTF)$_2$[Cu(NCS)$_2$] (H and D salts) [BEDT-TTF = bis(ethylenedithio)tetrathiafulvalene] were measured over the range from 500 to 28 000 cm^{-1} at room temperature with light polarizations parallel to the crystallographic b and c axes which lie on the two-dimensional conducting plane. Polarized reflectance spectra of the organic superconductor β-(BEDT-TTF)$_2$I$_3$ and the organic metal β''-(BEDT-TTF)$_2$AuBr$_2$ were also measured in order to discuss the influence of different molecular arrangements and hydrogen-anion contacts on the electronic and vibrational properties of these salts. Frequency-dependent conductivities were calculated by a Kramers-Kronig transformation. By comparison of the infrared conductivity spectra of the H and D salts, the vibrational transitions induced by electron–molecular-vibration (EMV) coupling were clearly distinguished from the carbon-hydrogen bending modes of the BEDT-TTF moiety. A Drude-Lorentz dielectric function was used to evaluate the optical transport parameters and an excitation frequency of the charge-transfer (CT) band superimposed on a plasma-edge-like dispersion which was observed for each compound. The EMV-coupling energies are semiquantitatively estimated to be ca. 70 meV for both the H and D salts from the frequencies of the EMV coupling transition and the CT band in terms of the dimer charge-oscillation model. By use of the coupling energy, various parameters describing the superconducting state were evaluated and discussed on the basis of the BCS theory in a weak-coupling limit. Finally, the magnitudes of hydrogen-anion interaction were estimated from the frequency shifts of the C—H bending modes of the BEDT-TTF moiety.

I. INTRODUCTION

The synthesis of a new class of organic superconductors having a novel structure has opened new perspectives in the field of organic superconductivity. The superconductors are κ-(BEDT-TTF)$_2$I$_3$,[1] κ-(BEDT-TTF)$_2$[Cu(NCS)$_2$],[2] the $r2$ (second rhombuslike crystal) modification of (DMET)$_2$AuBr$_2$,[3] and (MDT-TTF)$_2$AuI$_2$,[4] where BEDT-TTF, DMET, and MDT-TTF are bis(ethylenedithio)tetrathiafulvalene, dimethyl(ethylenedithio)diselenadithiafulvalene, and methylenedithiotatrathiafulvalene, respectively. These superconductors consist of two-dimensional conducting sheets of donor molecules with a zigzag arrangement of nearly eclipsed, face-to-face, molecular dimers. The dimers do not form stacking columns as found commonly in conventional organic conductors but form a two-dimensional interaction network where one molecular dimer is nearly perpendicular to each neighboring dimer. Since there is an unpaired electron per dimer, the dimer unit in the superconductors may be regarded as an atom having one valence electron like the alkali-metal elements. Therefore, the organic superconductors mentioned above are of great interest in the sense that they are expected to exhibit the rather isotropic nature of physical properties within the conducting sheet, because the dimer units, each having an unpaired electron, condense in a manner not to preserve the molecular anisotropy of the donors.

In this respect, these organic superconductors would exhibit physical properties like those in the layered compounds, such as transition-metal dichalcogenides.[5] In fact, we have previously shown that charge transport in the two-dimensional conducting sheet of κ-(BEDT-TTF)$_2$[Cu(NCS)$_2$] has a very small anisotropy not only in the dc conductivity[6] but also in the optical conductivity.[7] Similar results have recently been reported on κ-(BEDT-TTF)$_2$I$_3$.[8] Such a small optical anisotropy is in marked contrast to a large optical anisotropy observed in the conventional organic superconductors β-(BEDT-TTF)$_2X$ (X=I$_3$, IBr$_2$, and AuI$_2$).[9–16] This remarkable change in the optical anisotropy of the novel superconductors would result in their specific electronic properties.

Frequency-dependent conductivity (conductivity spectrum) is a useful tool to elucidate electronic properties of materials. Infrared conductivity spectra are of particular importance to discuss not only the transport nature but also the electron-phonon interaction in superconductors.

 ©1989 The American Physical Society

We have previously shown that for κ-(BEDT-TTF)$_2$[Cu(NCS)$_2$], the bands appearing in the frequency region between 1150 and 1320 cm^{-1} are possibly assigned as being due to C—H bending modes of the BEDT-TTF moiety.[7] However, the bands assigned to the C—H bending modes seem to superimpose on a strong broad band, which has been sometimes ascribed to the totally symmetric C=C stretching modes whose intensity is enhanced by the electron–molecular-vibration (EMV) (electron-phonon) interaction.[17,18] It is therefore necessary to substitute deuterium in place of the hydrogen of the BEDT-TTF moiety to distinguish the C—H bending bands from the C=C stretching band for the purpose of studying the electron-phonon interaction.

In this paper, we present the polarized reflectance spectra of protonated and deuterated κ-(BEDT-TTF)$_2$[Cu(NCS)$_2$] measured at room temperature. Infrared conductivity spectra are then obtained through a Kramers-Kronig transformation. By comparing the conductivity spectra of the protonated and deuterated salts, clear evidence for the EMV interaction is obtained. To acquire further insight into the EMV interaction, we also present the polarized reflectance and conductivity spectra of β-(BEDT-TTF)$_2$I$_3$ and β''-(BEDT-TTF)$_2$AuBr$_2$ and compared with those of κ-(BEDT-TTF)$_2$[Cu(NCS)$_2$]. Transport parameters for these salts are evaluated in terms of a Drude-Lorentz dielectric function and anisotropies of the transport parameters in the conducting BEDT-TTF sheet are discussed. The EMV coupling constants and energies for these BEDT-TTF salts are estimated in terms of the dimer charge-oscillation model.

II. EXPERIMENT

Single crystals, shaped like thin distorted hexagon plates, were prepared for α- and β-(BEDT-TTF)$_2$I$_3$ by the electrochemical oxidation of BEDT-TTF under galvanostatic conditions.[12] Single crystals of protonated and deuterated κ-(BEDT-TTF)$_2$[Cu(NCS)$_2$] (Refs. 2 and 7) and β''-(BEDT-TTF)$_2$AuBr$_2$ (Ref. 19) were kindly donated by Saito and Kobayashi, respectively.

The polarized reflectance spectra at nearly normal incidence were measured over the spectral range from 500 to 6000 cm^{-1} by using a Perkin-Elmer 1760 Fourier-transform infrared (FTIR) spectrometer equipped with a Spectra-Tech IR-PLAN$_{TM}$ microscope and a gold-wire-grid polarizer and measured over the range from 4000 to 28 000 cm^{-1} by using a home-made microspectrophotometer.[12] The Kramers-Kronig transformation was carried out with the modified-analysis method proposed by Ahrenkiel.[20]

III. RESULTS AND DISCUSSION

A. EMV-coupling modes

1. κ-(BEDT-TTF)$_2$[Cu(NCS)$_2$]

The crystal of deuterated κ-(BEDT-TTF)$_2$[Cu(NCS)$_2$] (D salt) exhibits a significant plasma-edge-like dispersion when the incident light, polarized parallel to the b axis, is irradiated onto the (100) crystal face, as shown in Fig. 1.[21] A similar dispersion is also observed for light polarized parallel to the c axis. These results indicate that there is little electronic anisotropy in the conducting sheet composed of BEDT-TTF species. The little anisotropy result has been previously shown by us[7] in the crystal of protonated κ-(BEDT-TTF)$_2$[Cu(NCS)$_2$] (H salt), and the spectra are shown in Fig. 2.[22] The reflectance spectra obtained for the H and D salts are approximately identical to each other except for the spectral region between 1000 and 1300 cm^{-1} in which C—H and C—D bending modes appear.[23]

The conductivity spectra obtained by the Kramers-Kronig transformation for the reflectance spectra with light polarized parallel to b and c exhibit several conductivity peaks as shown in Fig. 3 for the D salt and Fig. 4 for the H salt. To see the difference more clearly, the conductivity spectra of the H and D salts in the region from 500 to 2600 cm^{-1} are enlarged and compared to each other in Figs. 5 and 6 for the polarizations (P) parallel to b and c, respectively.

A significant difference between the conductivity spectra of the H and D salts is recognized in the region from 1000 to 1300 cm^{-1}, while a quite small difference is observed in the other infrared region. Frequencies of the conductivity peaks appearing in the infrared region are summarized in Table I together with those of the absorption bands observed in the crystals of protonated (h_8-) and deuterated (d_8-) BEDT-TTF.[24] In the H salt, sharp conductivity peaks appear at 1266 and 1171 cm^{-1} in the $P\|b$ spectrum and at 1292 and 1161 cm^{-1} in the $P\|c$ spectrum. Very strong broad peaks also appear in the same spectral region, i.e., at 1317 cm^{-1} for $P\|b$ and at 1209 cm^{-1} for $P\|c$. In the D salt the sharp peaks markedly shift toward the low-frequency side compared

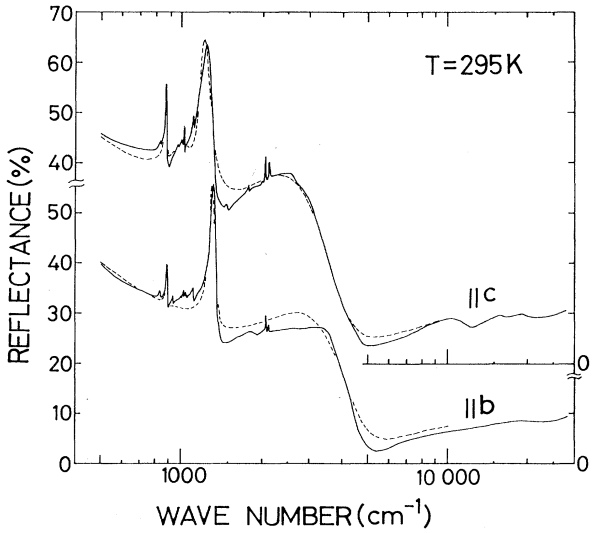

FIG. 1. Polarized reflectance spectra of the (100) crystal face of deuterated κ-(BEDT-TTF)$_2$[Cu(NCS)$_2$] at room temperature for polarizations parallel to the b and c axes. Least-squares fits to the reflectance assuming a Drude-Lorentz dielectric function are represented by dashed lines.

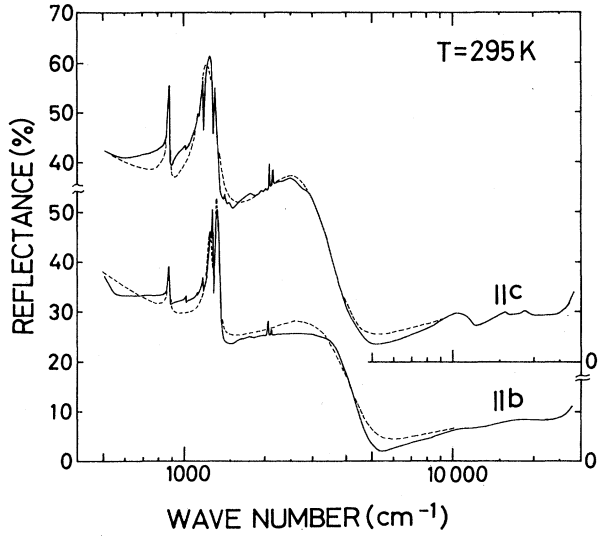

FIG. 2. Polarized reflectance spectra of the (100) crystal face of protonated κ-(BEDT-TTF)$_2$[Cu(NCS)$_2$] at room temperature for polarizations parallel to the b and c axis. Least-squares fits to the reflectance are represented by dashed lines.

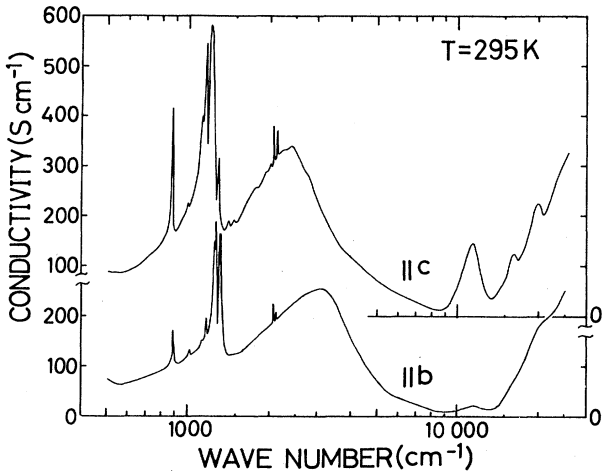

FIG. 4. Conductivity spectra of protonated κ-(BEDT-TTF)$_2$[Cu(NCS)$_2$] derived from the reflectance spectra by the Kramers-Kronig transformation.

with those of the H salt, whereas the broad peaks shift little. This clearly suggests that the sharp peaks are related to the vibrational modes of carbon-hydrogen bonds while the broad ones are not. The peaks at 1292, 1266, 1171, and 1161 cm^{-1} observed in the H salt are thus assigned to the C—H bending modes [δ(C—H)] of 1280, 1260, and 1170 cm^{-1} in the neutral h_8-BEDT-TTF, respectively. The peaks at 1112, 1026, 1019, and 1024 cm^{-1} observed in the D salt are also assigned to the C—D bending modes [δ(C—D)] of 1115, 1041, and 1015 cm^{-1} in the neutral d_8-BEDT-TTF. No infrared-active absorption corresponding to the intense broad peaks are observed in the spectra of neutral h_8- and d_8-BEDT-TTF.

The origin of the broad conductivity peaks located near 1200 and 1300 cm^{-1} would be due to the coupling of the conduction electrons to intramolecular vibrations of the BEDT-TTF species, i.e., EMV coupling. It is suggested that the intramolecular vibrational modes which couple with conduction electrons are the totally symmetric ones.[17,18,25] The frequency of the totally symmetric C=C stretching mode is observed in powder Raman spectra of protonated and deuterated κ-(BEDT-TTF)$_2$[Cu(NCS)$_2$] at 1472 and 1477 cm^{-1}, respectively.[26] It is known that the bare frequency of the C=C stretching mode, as observed in the Raman spectra of BEDT-TTF and TMTTF compounds, shifts downward by 100–200 cm^{-1} in the infrared spectra.[27,28] This leads us to assign the broad peaks at 1300 and 1317 cm^{-1} in the $P\|b$ spectra and at 1206 and 1209 cm^{-1} in the $P\|c$ spec-

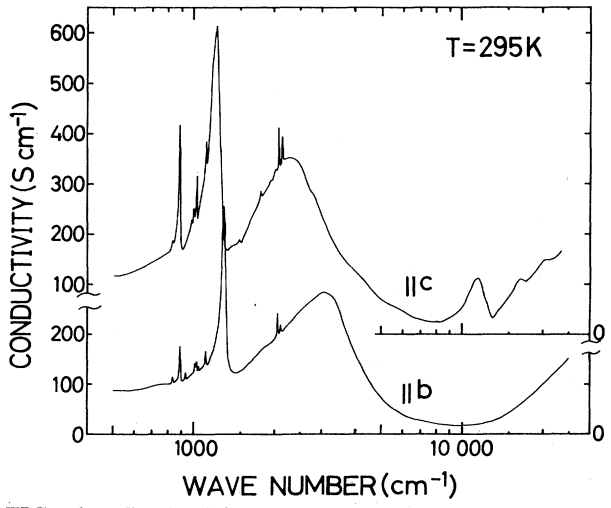

FIG. 3. Conductivity spectra of deuterated κ-(BEDT-TTF)$_2$[Cu(NCS)$_2$] derived from the reflectance spectra by the Kramers-Kronig transformation.

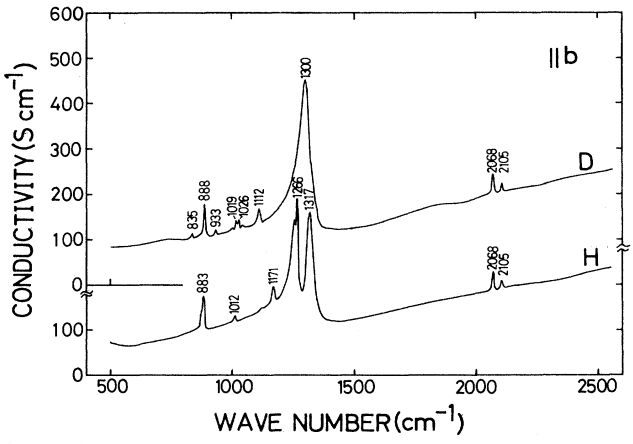

FIG. 5. Infrared conductivity spectra of protonated (H) and deuterated (D) κ-(BEDT-TTF)$_2$[Cu(NCS)$_2$] for the polarization parallel to the b axis.

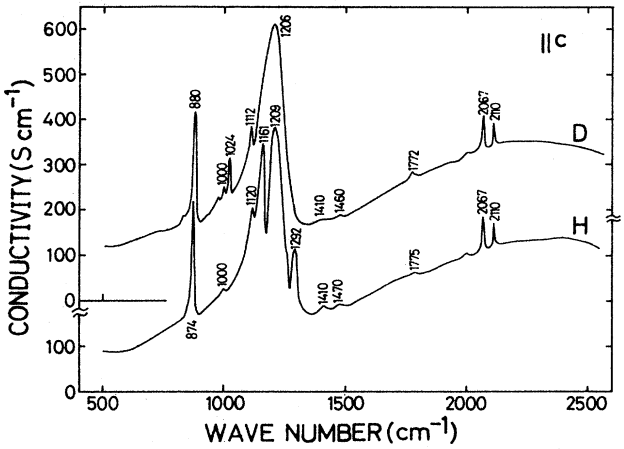

FIG. 6. Infrared conductivity spectra of protonated (H) and deuterated (D) κ-(BEDT-TTF)$_2$[Cu(NCS)$_2$] for the polarization parallel to the c axis.

tra to the coupling of electronic transitions to the C=C stretching mode. The difference in the frequency of the EMV coupled peaks in both polarization spectra will be discussed in Sec. III C.

The intense sharp peak near 880 cm^{-1} would be attributed to the totally symmetric C—S stretching of BEDT-TTF, the transition of which is also induced by the EMV interaction. In the same region, several infrared-active modes are observed in h_8- and d_8-BEDT-TTF as given in Table I. However, the peak near 880 cm^{-1} is too intense to be ascribed to the infrared-active modes. Since the totally symmetric C—S stretching mode appears in the Raman spectra at 876 cm^{-1} for h_8-BEDT-TTF,[28] 889 cm^{-1} for the H salt,[26] and 907 cm^{-1} for the D salt,[26] there is a possibility that the EMV coupling induces the transition due to the C—S mode near these frequencies. In fact, α-(BEDT-TTF)$_2$I$_3$ exhibits an intense absorption band at 877 cm^{-1} due to the EMV coupling without significant frequency reduction.[28] Therefore, the conductivity peaks at 883 and 874 cm^{-1} for the H salt and at 888 and 880 cm^{-1} for the D salt are assigned to the transition due to the C—S stretching mode of BEDT-TTF induced by the EMV interaction.

The remainder of conductivity peaks located in the region between 500 and 1600 cm^{-1} are ascribed to the vibrational modes of BEDT-TTF as shown in Table I. In the $P\|c$ spectra of both the H and D salts, the very weak peaks are observed at 1460–1470 and 1410 cm^{-1}. These peaks would be attributed to the infrared-active C=C stretching modes of BEDT-TTF, since the modes appear at 1505 and 1405 cm^{-1} in h_8-BEDT-TTF and at 1512

TABLE I. Infrared conductivity spectra (500–4000 cm^{-1}) of protonated (h_8-) and deuterated (d_8-) BEDT-TTF and protonated and deuterated κ-(BEDT-TTF)$_2$[Cu(NCS)$_2$] (H salt and D salt).[a] In parentheses are the transitions due to the totally symmetric modes induced by the electron—molecular-vibration coupling (see text).

		H salt				D salt	
h_8-BEDT-TTF[b] $\tilde{\nu}$ (cm^{-1})		$\|b$ $\tilde{\nu}$ (cm^{-1})	$\|c$ $\tilde{\nu}$ (cm^{-1})	d_8-BEDT-TTF[b] $\tilde{\nu}$ (cm^{-1})		$\|b$ $\tilde{\nu}$ (cm^{-1})	$\|c$ $\tilde{\nu}$ (cm^{-1})
2960 w 2920 w	ν(C—H)			2230 m 2177 w 2147 w	ν(C—D)		
			1775 vw				1772 vw
1505 w 1405 m	ν(C=C)		1470 vw 1410 vw	1512 m 1413 w	ν(C=C)		1460 vw 1410 vw
		(1317 vs)[c]	(1209 vs)[c]			(1300 vs)[c]	(1206 vs)[c]
1280 m 1260 w 1170 w	δ(C—H)	1266 s 1171 w	1292 m 1161 m	1115 m 1041 m 1015 m	δ(C—D)	1112 w 1026 w 1019 vw	1112 w 1024 w
1123 w			1120 vw				
995 w		1012 vw	1000 vw	991 w		1000 vw	1000 vw
915 sh				932 m		933 vw	975 sh
905 m				906 m			
		(883 m)[d]	(874 s)[d]			(888 m)[d]	(880 s)[d]
885 m				880 m			
868 m				826 w		835 vw	840 sh
				808 w			
				791 w			
770 s				770 s			
680 w				695 m			
ν(C≡N)							
(Cu-NCS-Cu)		2105 w	2110 w			2105 w	2110 w
(Cu-NCS)		2068 w	2067 w			2068 w	2067 w

[a]vs=very strong, s=strong, m=medium, w=weak, vw=very weak, sh=shoulder.
[b]Reference 24.
[c]The corresponding vibrations are observed at 1472 cm^{-1} for the H salt and 1477 cm^{-1} for the D salt in the Raman spectroscopy.
[d]The corresponding vibrations are observed at 889 cm^{-1} for the H salt and 907 cm^{-1} for the D salt in the Raman spectroscopy.

and 1413 cm^{-1} in d_8-BEDT-TTF. The higher-frequency mode shifts toward the low-frequency side by about 40 cm^{-1}. The frequency reduction of this size is probably due to the mixed-valence nature of the H and D salts because the frequency of the mode is known[29] to be 1445 cm^{-1} for a completely ionized BEDT-TTF salt, (BEDT-TTF)$_2$IBr$_2$(2IBr$_2$,C$_2$H$_3$Cl$_3$)$_{0.5}$.[30]

The sharp doublet peaks appearing at 2068 and 2105 cm^{-1} in the $P\|b$ spectra and at 2067 and 2110 cm^{-1} in the $P\|c$ spectra would be assigned to the C—N stretching modes of the $[Cu(NCS)_2]^-$ anion, because the deuterium substitution of BEDT-TTF moiety does not alter their frequencies while changing the frequencies of the other bands. The low- and high-energy bands are, respectively, attributed[7,31] to the C—N stretching modes of the N-bonded pendulous isothiocyanate and bridging isothiocyanate incorporated into the chain of the anions connected in the manner of [—Cu(NCS)—NCS—]$_n$.[32]

2. *β-(BEDT-TTF)$_2$I$_3$ and β″-(BEDT-TTF)$_2$AuBr$_2$*

As mentioned in the preceding section, in the infrared conductivity spectra of protonated κ-(BEDT-TTF)$_2$[Cu(NCS)$_2$], the EMV interaction induces the broad intense peak which is superimposed by several sharp peaks. An intense peak similar to this has previously been observed in β-(BEDT-TTF)$_2$I$_3$.[9–11,13,14] Insufficient resolution in the infrared region of the spectra reported for β-(BEDT-TTF)$_2$I$_3$, however, has hindered accurate analysis of the EMV interaction. We have therefore reexamined the polarized reflectance spectra with light $P\|a$ and $P\perp a$ in the (001) crystal face of β-(BEDT-TTF)$_2$I$_3$ with higher resolution (2–4 cm^{-1}) using the FTIR spectrometer. We have also measured the polarized reflectance spectra with light $P\|c$ and $P\perp c$ in the (010) crystal face of β″-(BEDT-TTF)$_2$AuBr$_2$ in order to compare the conductivity spectra of the organic superconductors with those of organic metals, since β″-(BEDT-TTF)$_2$AuBr$_2$ exhibits metallic behavior down to 6 K where a resistivity minimum is observed.[19,33]

The polarized reflectance spectra of β-(BEDT-TTF)$_2$I$_3$ and β″-(BEDT-TTF)$_2$AuBr$_2$ are shown in Figs. 7 and 8, respectively. The conductivity spectra were obtained by the Kramers-Kronig analysis. To compare the conductivity spectra of these salts with those of protonated κ-(BEDT-TTF)$_2$[Cu(NCS)$_2$], the spectra in the region between 500 and 2600 cm^{-1} are depicted in Fig. 9. The peak frequencies observed in the $P\|b$ and $P\|c$ spectra of the H salt, in the $P\|a$ and $P\perp a$ spectra of β-(BEDT-TTF)$_2$I$_3$, and in the $P\perp c$ spectrum of β″-(BEDT-TTF)$_2$AuBr$_2$ are listed in Table II. These spectra qualitatively look like one another except for the frequency region where the C—N stretching modes of $[Cu(NCS)_2]^-$ anion appear. This implies that the discussion described above for the H salt is applicable to β-(BEDT-TTF)$_2$I$_3$ and β″-(BEDT-TTF)$_2$AuBr$_2$.

According to the discussion in Sec. III A 1, the intense peaks appearing at 1230 cm^{-1} in the $P\|a$ and $P\perp a$ spectra of β-(BEDT-TTF)$_2$I$_3$ and at 1268 cm^{-1} in the $P\perp c$ spectrum of β″-(BEDT-TTF)$_2$AuBr$_2$ are attributed to the transition due to the totally symmetric C=C stretching mode induced by the EMV interaction. The peaks located at 875 cm^{-1} for β-(BEDT-TTF)$_2$I$_3$ and at 880 cm^{-1} for β″-(BEDT-TTF)$_2$AuBr$_2$ are assigned to the transition due to the totally symmetric C—S stretching mode also induced by the EMV interaction. The remainder conductivity peaks are ascribed to the infrared-active modes of h_8-BEDT-TTF as shown in Table II. In conclusion, it is found that there is no significant difference among the vibrational properties of these BEDT-TTF salts in spite of their scattered nature of transport properties ranging from superconducting to metallic.

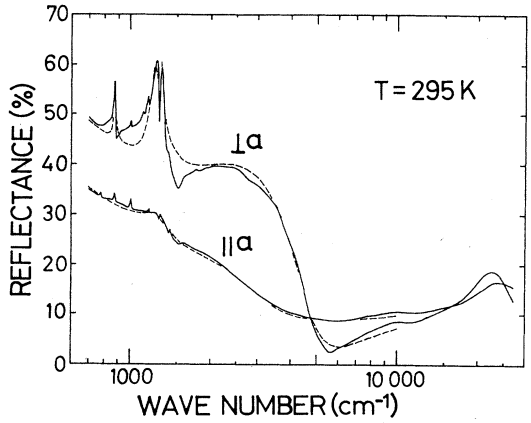

FIG. 7. Polarized reflectance spectra of the (001) crystal face of β-(BEDT-TTF)$_2$I$_3$ at room temperature for polarizations parallel and perpendicular to the a axis. Least-squares fits to the reflectance are represented by dashed lines.

B. Electronic transitions and transport properties

The plasma-edge-like dispersion observed in the reflectance spectra of protonated and deuterated κ-(BEDT-TTF)$_2$[Cu(NCS)$_2$], β-(BEDT-TTF)$_2$I$_3$, and β″-

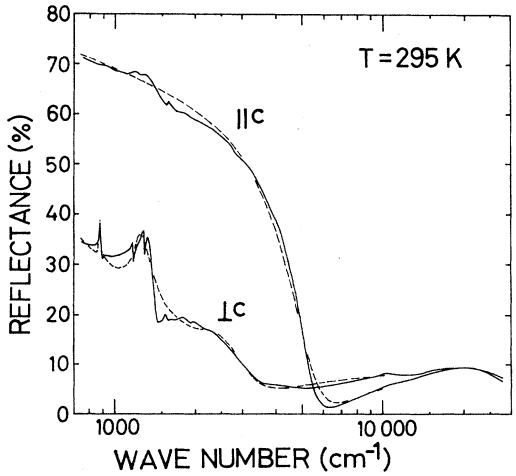

FIG. 8. Polarized reflectance spectra of the (010) crystal face of β″-(BEDT-TTF)$_2$AuBr$_2$ at room temperature for polarizations parallel and perpendicular to the c axis. Least-squares fits to the reflectance are represented by dashed lines.

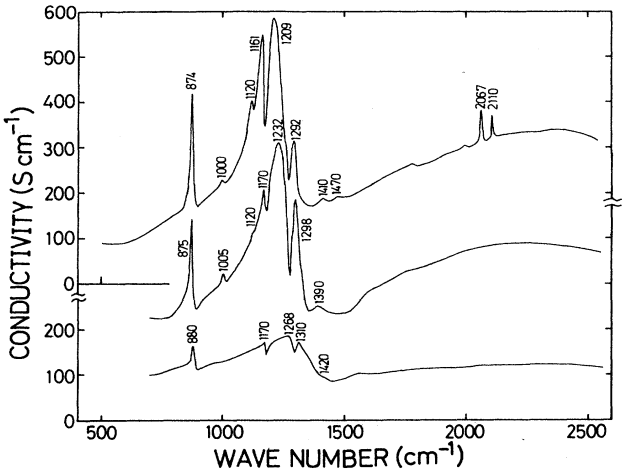

FIG. 9. Infrared conductivity spectra of protonated κ-(BEDT-TTF)$_2$[Cu(NCS)$_2$] for polarization parallel to the c axis (top), β-(BEDT-TTF)$_2$I$_3$ for polarization perpendicular to the a axis (middle), and β''-(BEDT-TTF)$_2$AuBr$_2$ for polarization perpendicular to the c axis (bottom).

(BEDT-TTF)$_2$AuBr$_2$ seem to deviate from Drude behavior except for the $P\|c$ spectrum of β''-(BEDT-TTF)$_2$AuBr$_2$. The conductivity spectra of these salts exhibit a broad peak around 2500 cm^{-1}. This implies the presence of some electronic transitions in the infrared frequency region. Of course, intense oscillators due to the vibrational bands induced by the EMV interaction also yield the deviation from simple Drude behavior. We have, therefore, analyzed the dispersion by fitting it to the reflectance calculated in terms of the frequency-dependent dielectric function $\epsilon(\omega)$ on the basis of the Drude-Lorentz oscillator model,

$$\epsilon(\omega)=\epsilon_{\text{core}}-\omega_p^2[\omega^2+i(\omega/\tau)]^{-1}+(4\pi ne^2/m)\sum_j f_j(\omega_j^2-\omega^2-i\Gamma_j\omega)^{-1}, \quad (1)$$

where ω_p is the plasma frequency, ϵ_{core} the dielectric constant at high frequency, and τ the relaxation time of carriers. The subscript j stands for the jth Lorentz oscillator with oscillator strength f_j. The best-fit curves are drawn by broken lines in Figs. 1, 2, 7, and 8, and the transport parameters obtained are summarized in Table III together with the valence-electron density n and the optical mass m_o derived from the fitting parameter.

The optical mass of κ-(BEDT-TTF)$_2$[Cu(NCS)$_2$] has a small anisotropy in the conducting bc plane; $m_o^{\|b}/m_o^{\|c}=1.3$ for the H salt and 1.4 for the D salt. The small anisotropy is in contrast with a large anisotropy $m_o^{\perp c}/m_o^{\|c}=4.5$ obtained in the conducting ac plane of β''-(BEDT-TTF)$_2$AuBr$_2$. The large optical anisotropy of the latter salt is consistent with an open Fermi surface for the hole band calculated for β''-(BEDT-TTF)$_2$AuBr$_2$ though a closed hole pocket coexists.[19,34] An optical anisotropy $m_o^{\|a}/m_o^{\perp a}=1.8$ obtained[35] in the conducting ab plane of β-(BEDT-TTF)$_2$I$_3$ is an intermediate between the anisotropies of κ-(BEDT-TTF)$_2$[Cu(NCS)$_2$] and β''-(BEDT-TTF)$_2$AuBr$_2$. This result agrees with a closed Fermi surface calculated for β-(BEDT-TTF)$_2$I$_3$,[36,37] while open surfaces have been recently reported.[38]

It is worth noting that the ratios of optical mass to the electron rest mass m_o/m are 3.2–4.6 and agree well with those of cyclotron masses $m_c/m=3.5$ for the H salt[39] and

TABLE II. Infrared conductivity spectra (500–2500 cm^{-1}) of protonated (h_8-) BEDT-TTF, protonated κ-(BEDT-TTF)$_2$[Cu(NCS)$_2$] (H salt), β-(BEDT-TTF)$_2$I$_3$, and β''-(BEDT-TTF)$_2$AuBr$_2$.[a] In parentheses are the transitions due to the totally symmetric modes induced by the electron–molecular-vibration coupling (see text).

	H salt		β-(BEDT-TTF)$_2$I$_3$		β''-(BEDT-TTF)$_2$AuBr$_2$
h_8-BEDT-TTF[b]	$\|b$	$\|c$	$\|a$	$\perp a$	$\perp c$
$\tilde{\nu}$ (cm^{-1})	$\tilde{\nu}$ (cm^{-1})	$\tilde{\nu}$ (cm^{-1})	$\tilde{\nu}$ (cm^{-1})	$\tilde{\nu}$ (cm^{-1})	$\tilde{\nu}$ (cm^{-1})
1505 w, 1405 m ν(C=C)		1470 vw			
		1410 vw	1410 vw	1390 w	1420 w
	(1317 vs)[c]	(1209 vs)[c]	(1230 w)[c]	(1232 vs)[c]	(1268 s)[c]
1280 m, 1260 w, 1170 w δ(C—H)		1292 m	1304 vw	1298 m	1310 w
	1266 s				
	1171 w	1161 m	1170 vw	1170 w	1170 w
1123 w		1120 vw		1120 sh	
995 w	1012 vw	1000 vw	1004 w	1005 vw	
915 sh					
905 m					
	(883 m)[d]	(874 s)[d]	(875 w)[d]	(875 s)[d]	(880 m)[d]
885 m					
868 m					
770 s			775 w		

[a]vs=very strong, s=strong, m=medium, w=weak, vw=very weak, sh=shoulder.
[b]Reference 24.
[c]The corresponding vibration is observed at 1472 cm^{-1} for the H salt and 1468 cm^{-1} for β-(BEDT-TTF)$_2$I$_3$ in the Raman spectroscopy.
[d]The corresponding vibration is observed at 889 cm^{-1} for the H salt in the Raman spectroscopy.

TABLE III. Transport parameters obtained from the Drude-Lorentz analyses of the polarized reflectance spectra of protonated and deuterated κ-(BEDT-TTF)$_2$[Cu(NCS)$_2$] (H and D salts), β-(BEDT-TTF)$_2$I$_3$, and β''-(BEDT-TTF)$_2$AuBr$_2$.

	$\omega_p/2\pi c$ (cm^{-1})	τ (10^{-15} s)	m_o/m	n (10^{21} cm^{-3})
H salt				
$\|b$	4950	1.14	4.3	1.18
$\|c$	5710	1.08	3.2	1.18
D salt				
$\|b$	4810	1.40	4.6	1.19
$\|c$	5660	1.30	3.3	1.19
β-(BEDT-TTF)$_2$I$_3$				
$\|a$	4490	1.42	5.2	1.17
$\perp a$	6020	1.90	2.9	1.17
β''-(BEDT-TTF)$_2$AuBr$_2$				
$\|c$	10040	2.27	1.1	1.23
$\perp c$	4730	1.61	4.9	1.23

3.4 for the D salt[40] which are determined by Shubnikov–de Haas effect measurements. In contrast, m_c/m determined for β-(BEDT-TTF)$_2$I$_3$ by Shubnikov–de Haas measurements is 0.4–0.5 (Ref. 41) and is about one order of magnitude smaller than the values of m_o/m obtained from the reflectance spectra. This discrepancy is, however, not surprising because m_c is dependent on the cross-sectional area of the Fermi surface, while m_o is related to the dispersion of the energy band. These two kinds of effective mass should coincide with each other when the energy band is described by a free-electron approximation. Therefore, remarkable similarity between m_o and m_c in κ-(BEDT-TTF)$_2$[Cu(NCS)$_2$] seems to indicate free-electron-like behavior of conduction electrons in this salt. Approximately temperature-independent paramagnetic susceptibility in the normal state of κ-(BEDT-TTF)$_2$[Cu(NCS)$_2$] (Refs. 2 and 42) is consistent with the free-electron-like behavior.

Now let us turn to the discussion of Lorentz oscillators. As shown in Table IV, there are two types of oscillators; one is associated with a small oscillator strength (less than 0.03) and the other is associated with a large oscillator strength (around 0.3). The former is due to the vibrational transitions induced by the EMV interaction as described above. The latter would be attributed to the electronic transition having the nature of charge-transfer (CT) excitation within the dimer consisting of BEDT-TTF moieties, because the oscillator strength obtained here is greater for the polarization parallel to the direction connecting molecular centers within the dimer than for the polarization perpendicular to this direction.[19,32–34,43] The broad conductivity peak around 2500 cm^{-1} appearing in some BEDT-TTF salts has been ascribed to interband transitions within a one-electron band model.[44,45] The interband transition appears in the BEDT-TTF salts in which BEDT-TTF forms a dimeric arrangement, whereas it is hardly observed for the BEDT-TTF salts with regular molecular arrays. This

TABLE IV. Transition frequencies ω_j (cm^{-1}), damping factors Γ_j (cm^{-1}), and oscillator strengths f_j of the jth vibrational modes. Those of the charge-transfer band are denoted by ω_{CT}, Γ_{CT}, and f_{CT}, and the dielectric constant at high frequency is represented by ϵ_{core}. Abbreviations for the salts are the same as used in Table III.

	H salt		D salt		β-(BEDT-TTF)$_2$I$_3$		β''-(BEDT-TTF)$_2$AuBr$_2$	
	$\|b$	$\|c$	$\|b$	$\|c$	$\|a$	$\perp a$	$\|c$	$\perp c$
ω_1	880	871	887	879		870		878
Γ_1	16	16	7	12		16		10
f_1	0.002	0.0006	0.002	0.0003		0.001		0.0002
ω_2	1253			1020	1230	1218		1230
Γ_2	52			180	260	92		180
f_2	0.007			0.009	0.003	0.02		0.007
ω_3	1321	1185	1300	1204		1302		
Γ_3	24	117	41	67		14		
f_3	0.003	0.032	0.009	0.022		0.001		
ω_{CT}	2910	2390	2890	2320	2450	2450		2500
Γ_{CT}	2280	1480	2240	1670	2780	2330		1230
f_{CT}	0.29	0.23	0.32	0.24	0.08	0.34		0.04
ϵ_{core}	3.3	3.9	3.6	3.9	3.6	3.6	3.4	3.4

fact indicates that the interband transition is attributable to the transition between the split energy bands, which results from the strong interaction within the dimer.[45] In a localized electron scheme, the interband transition could therefore be regarded as CT within the dimer. Thus, we describe the frequency of the oscillator as the transition frequency of the CT excitation within the dimer ω_{CT}.

Before concluding this section, it may be appropriate to make comments on the remainder conductivity peaks in the visible region. In the $P\|c$ spectra of protonated and deuterated κ-(BEDT-TTF)$_2$[Cu(NCS)$_2$], three peaks are superimposed on a broad conductivity background as shown in Figs. 3 and 4. The peaks would be assigned to the intramolecular excitations of BEDT-TTF cation radical as discussed below. The conductivity spectrum of α-(BEDT-TTF)$_2$I$_3$ obtained from the polarized reflectance spectrum measured with light polarization parallel to the c^* direction, which is nearly parallel to the molecular long axis of BEDT-TTF,[46] exhibits an intense peak at 9700 cm^{-1} and weak peaks at 16 000 and 20 000 cm^{-1} as shown in Fig. 10. The CT interaction along the c^* direction is expected to be weak compared with that along the conducting *ab* plane because of insertion of the tri-iodide anion sheet between the BEDT-TTF sheets.[46] Thus, the low-lying excitation of these three peaks could not be attributed to a CT transition. The three peaks therefore should be assigned to the intramolecular excitation of BEDT-TTF cation radical, which are polarized along the long axis of the molecule. The peaks appearing in the $P\|c$ spectrum of κ-(BEDT-TTF)$_2$[Cu(NCS)$_2$] are located at 11 400, 16 100, and 19 900 cm^{-1}. These excitation energies are close to those observed in α-(BEDT-TTF)$_2$I$_3$. In addition, the peaks are hardly observed in the $P\|b$ spectrum, where the polarization direction is perpendicular to the molecular long axis of BEDT-TTF.[7,32] The energies and polarization of the conductivity peaks observed in κ-(BEDT-TTF)$_2$[Cu(NCS)$_2$] thus indicate that the peaks are to be assigned to the intramolecular transitions of BEDT-TTF cation radical.

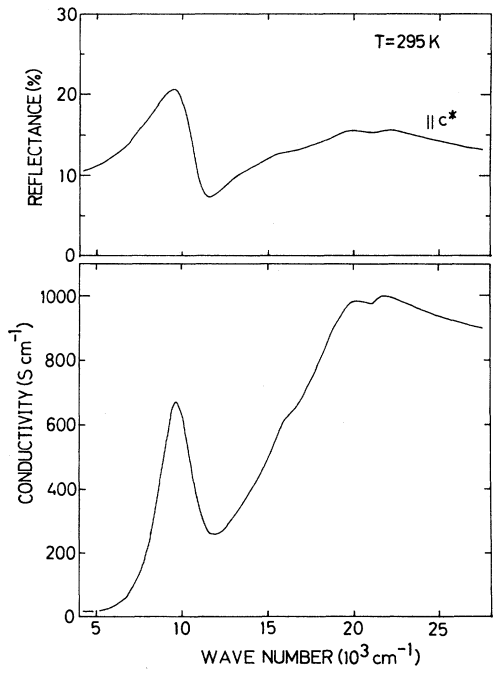

FIG. 10. Polarized reflectance (upper) and conductivity (lower) spectra of α-(BEDT-TTF)$_2$I$_3$ at room temperature for polarization parallel to the c^* direction (nearly parallel to the molecular long axis of BEDT-TTF moiety).

C. EMV coupling and superconductivity in the salts

As shown in Sec. III A, there is considerable interaction between the conduction electrons and molecular-vibrational modes, i.e., the EMV coupling, in κ-(BEDT-TTF)$_2$[Cu(NCS)$_2$], β-(BEDT-TTF)$_2$I$_3$, and β''-(BEDT-TTF)$_2$AuBr$_2$. As also shown in Sec. III B, the CT band, closely related to the BEDT-TTF dimer, is observed in these salts. These results suggest that we analyze the EMV coupling in terms of the dimer charge-oscillation model.[17,18,27,28]

According to this model, if the bare frequency ω of the EMV coupled mode is well separated from the frequencies of other vibrational modes and the EMV coupling constant λ is sufficiently small, λ may be evaluated by using the following equation

$$(\omega^2-\Omega^2)/\omega^2=\lambda\omega_{CT}^2/(\omega_{CT}^2-\omega^2)\ , \tag{2}$$

where Ω is the observed frequency of the EMV coupled mode and ω_{CT} is the frequency of the CT transition.[27] We can identify ω with the Raman frequency of the totally symmetric C=C stretching mode, Ω with the frequency of the transition due to the C=C stretching mode induced by the EMV interaction, and ω_{CT} with the frequency of the electronic transition observed in the infrared region, as noted in Secs. III A and III B. With the values listed in Table V, λ is obtained to be 0.15 ($P\|b$) and 0.20 ($P\|c$) for the H salt, 0.17 ($P\|b$) and 0.20 ($P\|c$) for the D salt, 0.19 for β-(BEDT-TTF)$_2$I$_3$, and 0.17 for β''-(BEDT-TTF)$_2$AuBr$_2$. For the AuBr$_2$ salt $\omega/2\pi_c$ is assumed to be 1470 cm^{-1} as being similar to that for the other h_8-BEDT-TTF based salts, since the experimental value is not available.

The EMV coupling energy g is related to λ by the equation,[27]

$$g=(\omega\lambda\omega_{CT}/2)^{1/2}\ . \tag{3}$$

By using the values of λ deduced from Eq. (2), values of g in the range 70–74 meV are obtained for the H salt and 72–74 meV for the D salt as shown in Table V. This result indicates that there is no significant difference between the coupling energies deduced from both the $P\|b$ and $P\|c$ spectra, whereas clear difference is recognized in the frequencies of the EMV coupled peaks as pointed out in Sec. III A 1. The difference in the coupled frequency could result from the difference in ω_{CT} taking account of Eqs. (2) and (3). Therefore, there is no substantial difference between the coupling energies obtained for the H and D salts. Furthermore, the coupling energies for β-(BEDT-TTF)$_2$I$_3$ and β''-(BEDT-TTF)$_2$AuBr$_2$ are also

TABLE V. Electron–molecular-vibration coupling constant λ and energy g, frequency of the charge-transfer transitions ω_{CT}, and bare and coupled totally symmetric mode frequencies ω and Ω. Abbreviations for the salts are the same as used in Table III.

	H salt		D salt			
	$\|b$	$\|c$	$\|b$	$\|c$	β-(BEDT-TTF)$_2$I$_3$	β''-(BEDT-TTF)$_2$AuBr$_2$
$\omega_{CT}/2\pi c$ (cm^{-1})	2910	2390	2890	2320	2450	2500
$\omega/2\pi c$ (cm^{-1})	1472		1477		1468	(1470)[a]
$\Omega/2\pi c$ (cm^{-1})	1317	1209	1300	1206	1230	1268
λ	0.15	0.20	0.17	0.20	0.19	0.17
g (meV)	70	74	74	72	73	69

[a]ω for β''-(BEDT-TTF)$_2$AuBr$_2$ is assumed to be similar to that for the other h_8-BEDT-TTF based salts since the experimental value is not available.

very close to those for the H and D salts as shown in Table V. Close similarity in the EMV coupling energy suggests again that there is no significant difference among the vibrational properties of these three BEDT-TTF salts in spite of their scattered electronic properties.

It is probably pertinent to discuss the relation between the EMV coupling energy and the superconducting nature of κ-(BEDT-TTF)$_2$[Cu(NCS)$_2$] because the EMV coupling has been suggested to be a possible mechanism of the electron-phonon interaction responsible for superconductivity.[47] If the coupling energy g is assumed to be the electron-phonon interaction energy, the BCS theory for a weak-coupling limit $gN(E_F) \ll 1$ predicts the critical temperature as

$$T_c = 1.134\Theta_D \exp\{-[gN(E_F)]^{-1}\} , \quad (4)$$

where Θ_D is the Debye temperature and $N(E_F)$ is the density of states at the Fermi level. We have previously shown that $N(E_F)$ can be estimated from the paramagnetic susceptibility in the normal state of κ-(BEDT-TTF)$_2$[Cu(NCS)$_2$] because of its approximately temperature-independent, i.e., Pauli, paramagnetism.[42] Using the values $g=70$ meV and $N(E_F)=7.1$ eV^{-1} per formula unit, the electron-phonon interaction parameter $gN(E_F)=0.50$ is obtained. This value is close to 0.4 reported for aluminum, a prototype of a weak coupler.[48] In addition, we have shown that the critical fields obtained from the field dependence of *ac* susceptibility yield a thermodynamically consistent picture when they are analyzed in terms of the anisotropic effective-mass model for the Ginzburg-Landau theory with a weak-coupling BCS gap.[21,49] These facts allow us to use the weak-coupling BCS equation (4).

By combining $gN(E_F)=0.50$ with $T_c=10.4$ K, $\Theta_D=68$ K is obtained. This value is comparable substantially to $\Theta_D=36$ K derived very recently from the phonon contribution to the heat capacity of κ-(BEDT-TTF)$_2$[Cu(NCS)$_2$].[50] The electronic contribution to the heat capacity γ is also evaluated to be less than 5 mJ mol^{-1} K^{-2}.[50] This value is, however, about seven times as small as 35.4 mJ mol^{-1} K^{-2} calculated from $N(E_F)=2.82\times10^{43}$ J^{-1} mol^{-1} with the equation,

$$\gamma = (2/3)\pi^2 N(E_F) k_B^2 , \quad (5)$$

where k_B is the Boltzmann constant.

Similar analysis for β-(BEDT-TTF)$_2$I$_3$ yields $\Theta_D=49$ K and $\gamma=33.2$ mJ mol^{-1} K^{-2} from Eqs. (4) and (5) with $g=73$ meV, $N(E_F)=7.1$ eV^{-1} or $=2.65\times10^{43}$ J^{-1} mol^{-1},[51] and $T_c=8$ K.[52–54] These values may be compared with the observed values of $\Theta_D=197$ K and $\gamma=24$ mJ mol^{-1} K^{-2}.[55] At the present stage, there is, therefore, no overall consistency among the parameters derived optically, magnetically, and thermodynamically within the BCS theory in the weak-coupling limit.

D. Cation-anion interaction and the C—H bending modes

Besides the EMV coupling, the cation-anion interaction through the hydrogen-anion contacts in the organic solids is pointed out to play a crucial role in determining the physical properties, especially T_c of the superconductors β-(BEDT-TTF)$_2X$ (X=I$_3$, IBr$_2$, and AuI$_2$).[56] The inverse isotope effect on T_c ($\Delta T_c/T_c=0.06$) observed for κ-(BEDT-TTF)$_2$[Cu(NCS)$_2$] is tentatively ascribed to the change in electron-phonon coupling due to the hydrogen-anion contacts.[6,57] In this section we therefore describe comparatively the influence of hydrogen-anion contacts on the frequency of C—H bending modes observed in the salts.

The frequency of a bending mode shifts to a higher frequency than that of a molecule in the absence of contact (or H bonding), while it displays no obvious change in half-width and absorption coefficient.[58] As seen in Table II, the highest-frequency vibration of the C—H bending modes observed in κ-(BEDT-TTF)$_2$[Cu(NCS)$_2$], β-(BEDT-TTF)$_2$I$_3$, and β''-(BEDT-TTF)$_2$AuBr$_2$ shifts to the higher-frequency side. This indicates that there is considerable cation-anion interaction through the hydrogen-anion contacts in all the salts as previously pointed out by the structural feature except for the AuBr$_2$ salt. In β-(BEDT-TTF)$_2$I$_3$ intermolecular H $\cdots$ I contact distances of 2.842 and 2.988 Å, shorter than the sum of van der Waals radii ($S_{HI}=3.35$ Å), are reported by means of the neutron diffraction at 20 K.[59] In κ-(BEDT-TTF)$_2$[Cu(NCS)$_2$] intermolecular H $\cdots$ N contact distances of 2.46 and 2.59 Å ($S_{HN}=2.7$ Å) and H $\cdots$ S distances of 2.84, 2.84, and 2.87 Å ($S_{HS}=3.05$ Å) are obtained through x-ray diffraction at 104 K.[32]

The amount of frequency shift increases in the order of κ-(BEDT-TTF)$_2$[Cu(NCS)$_2$] $<\beta$-(BEDT-TTR)$_2$I$_3$ $<\beta''$-(BEDT-TTF)$_2$AuBr$_2$. The cation-anion interaction is probably enhanced in this order. However, direct com-

parison among the frequency shifts in these salts is not appropriate because the different element atoms (i.e., N and S in the $[Cu(NCS)_2]$ salt, I in the I_3 salt, and Br in the $AuBr_2$ salt) are incorporated in the contact with the hydrogen atoms. In the present state we can only suggest that there is a considerable amount of hydrogen-anion interaction in these BEDT-TTF salts. The spectral evidence for the hydrogen-anion interaction is shown here for the first time by the analysis of the infrared conductivity spectra.

On the other hand, the highest frequency of the C—D bending mode observed in deuterated κ-(BEDT-TTF)$_2$[Cu(NCS)$_2$] scarcely shifts from that reported on d_8-BEDT-TTF. This implies that the cation-anion interaction in the D salt is not obvious compared with that in the H salt. To date, however, deuterium-anion contact distances in the D salt are not known and structural information on the cation-anion interaction is not available. To acquire structural insight into the cation-anion interaction, x-ray structure analysis of the D salt is currently in progress.

IV. CONCLUSIONS

The detailed analysis of the polarized reflectance spectra of the ambient-pressure organic superconductors protonated and deuterated κ-(BEDT-TTF)$_2$[Cu(NCS)$_2$] has yielded an unambiguous identification of spectroscopic feature originated from the EMV interaction and their assignment to specific molecular normal modes. The results show that the modes exhibiting the strongest coupling with electrons are the totally symmetric C=C and C—S stretching modes. By using this identification and assignment, the EMV interaction in the ambient-pressure organic superconductor β-(BEDT-TTF)$_2$I$_3$ and the organic metal β''-(BEDT-TTF)$_2$AuBr$_2$ has also been discussed. It is shown that there is no significant difference among the vibrational properties of these BEDT-TTF salts in spite of their scattered transport properties ranging from superconducting to metallic.

The analysis has also yielded the fact that the anisotropy of optical mass in the two-dimensionally connected molecular sheets of BEDT-TTF moieties in these salts varies in the order κ-(BEDT-TTF)$_2$[Cu(NCS)$_2$] < β-(BEDT-TTF)$_2$I$_3$ < β''-(BEDT-TTF)$_2$AuBr$_2$; namely κ-(BEDT-TTF)$_2$[Cu(NCS)$_2$] has the largest two dimensionality in optical transport. This result is consistent with the structural feature of the $[Cu(NCS)_2]$ salt in which the BEDT-TTF dimers condense in a manner not to preserve their molecular anisotropy.

The semiquantitative estimation of the EMV coupling energies as well as coupling constants in terms of the dimer charge-oscillation model give a substantially similar coupling energy near 70 meV for all the salts. Application of the BCS theory in a weak-coupling limit because of the small electron-phonon interaction parameter 0.50 deduced from the EMV coupling energy has provided the Debye temperature of about 70 K, which is comparable to that derived from the phonon contribution of heat capacity. From the frequency shifts of the C—H and C—D bending modes, it is suggested that the hydrogen-anion interaction is considerably large in the protonated BEDT-TTF salts while negligibly small in the deuterated compound.

ACKNOWLEDGMENTS

The authors are indebted to Professor G. Saito of the Institute for Solid State Physics for kindly providing the crystals of protonated and deuterated κ-(BEDT-TTF)$_2$[Cu(NCS)$_2$] and to Professor H. Kobayashi of Toho University for kindly donating the crystals of β''-(BEDT-TTF)$_2$AuBr$_2$. This work was in part supported by a Grant-in-Aid for the Scientific Research from the Ministry of Education, Science, and Culture, Japan.

[1]A. Kobayashi, R. Kato, H. Kobayashi, S. Moriyama, Y. Nishio, K. Kajita, and W. Sasaki, Chem. Lett. **1987**, 459 (1987).

[2]H. Urayama, H. Yamochi, G. Saito, K. Nozawa, T. Sugano, M. Kinoshita, S. Sato, K. Oshima, A. Kawamoto, and J. Tanaka, Chem. Lett. **1988**, 55 (1988).

[3]K. Kikuchi, Y. Honda, Y. Ishikawa, K. Saito, I. Ikemoto, K. Murata, H. Anzai, T. Ishiguro, and K. Kobayashi, Solid State Commun. **66**, 405 (1988).

[4]G. C. Papavassiliou, G. A. Mousdis, J. S. Zambounis, A. Terzis, A. Hountas, B. Hilti, C. W. Mayer, and J. Pfeiffer, Synth. Metals **27**, B379 (1988).

[5]See, for example, J. A. Wilson, F. J. DiSalvo, and S. Mahajan, Adv. Phys. **24**, 117 (1975).

[6]K. Oshima, H. Urayama, H. Yamochi, and G. Saito, J. Phys. Soc. Jpn. **57**, 730 (1988).

[7]T. Sugano, H. Hayashi, H. Takenouchi, K. Nishikida, H. Urayama, H. Yamochi, G. Saito, and M. Kinoshita, Phys. Rev. B **37**, 9100 (1988).

[8]M. Tamura, K. Yakushi, H. Kuroda, R. Kato, H. Kobayashi, and A. Kobayashi, in Abstracts of 56th Annual Meeting of the Chemical Society of Japan, Tokyo, 1988 (unpublished), p. 122.

[9]R. M. Vlasova, E. A. Ivanova, and V. N. Semkin, Sov. Phys. Solid State **27**, 326 (1985).

[10]B. Koch, H. P. Geserich, W. Ruppel, D. Schweitzer, K. H. Dietz, and H. J. Keller, Mol. Cryst. Liq. Cryst. **119**, 343 (1985).

[11]C. S. Jacobsen, J. M. Williams, and H. H. Wang, Solid State Commun. **54**, 937 (1985).

[12]T. Sugano, K. Yamada, G. Saito, and M. Kinoshita, Solid State Commun. **55**, 137 (1985).

[13]M. G. Kaplunov, E. B. Yagubskii, L. P. Rosenberg, and Yu. G. Borodko, Phys. Status Solidi A **89**, 509 (1985).

[14]H. Tajima, K. Yakushi, H. Kuroda, and G. Saito, Solid State Commun. **56**, 159 (1985).

[15]T. Sugano and G. Saito, J. Phys. C **19**, 5471 (1986).

[16]C. S. Jacobsen, D. B. Tanner, J. M. Williams, U. Geiser, and H. H. Wang, Phys. Rev. B **35**, 9605 (1987).

[17]M. J. Rice, Phys. Rev. Lett. **37**, 36 (1976).

[18]N. O. Lipari, C. B. Duke, R. Bozio, A. Girland, C. Pecile, and A. Padova, Chem. Phys. Lett. **44**, 236 (1976).
[19]K. Kajita, Y. Nishio, S. Moriyama, W. Sasaki, R. Kato, H. Kobayashi, and A. Kobayashi, Solid State Commun. **60**, 811 (1986).
[20]R. K. Ahrenkiel, J. Opt. Soc. Am. **61**, 1651 (1971).
[21]Preliminary results for the D salt was reported in T. Sugano, K. Nozawa, H. Hayashi, K. Nishikida, K. Terui, T. Fukasawa, H. Takenouchi, S. Mino, H. Urayama, H. Yamochi, G. Saito, and M. Kinoshita, Synth. Metals **27**, A325 (1988).
[22]Similar spectra with low resolution for the crystals of H salt prepared in a different manner were reported in A. Ugawa, G. Ojima, K. Yakushi, and H. Kuroda, Phys. Rev. B **38**, 5122 (1988).
[23]Similar spectra for the crystals of D salt were reported independently in M. Tokumoto, H. Anzai, K. Takahashi, N. Kinoshita, K. Murata, T. Ishiguro, Y. Tanaka, Y. Hayakawa, H. Nagamori, and K. Nagasaka, Synth. Metals **27**, A171 (1988).
[24]H. H. Wang, P. E. Reed, and J. M. Williams, Synth. Metals **14**, 165 (1986).
[25]C. B. Duke, Ann. N.Y. Acad. Sci. **313**, 166 (1978).
[26]S. Sugai (private communication).
[27]R. Bozio, M. Meneghetti, and C. Pecile, J. Chem. Phys. **76**, 5785 (1982).
[28]M. Meneghetti, R. Bozio, and C. Pecile, J. Phys. (Paris) **47**, 1377 (1986).
[29]H. Hayashi, T. Sugano, and M. Kinoshita (unpublished).
[30]H. Yamochi, H. Urayama, G. Saito, K. Oshima, A. Kawamoto, and J. Tanaka, Chem. Lett. **1988**, 1211 (1988).
[31]K. Nakamoto, *Infrared and Raman Spectra of Inorganic and Coordination Compounds,* 4th ed. (Wiley, New York, 1986), p. 283.
[32]H. Urayama, H. Yamochi, G. Saito, S. Sato, A. Kawamoto, J. Tanaka, T. Mori, Y. Maruyama, and H. Inokuchi, Chem. Lett. **1988**, 463 (1988).
[33]M. Kurmoo, D. R. Talham, P. Day, I. D. Parker, R. H. Friend, A. M. Stringer, and J. A. K. Howard, Solid State Commun. **61**, 459 (1987).
[34]T. Mori, F. Sakai, G. Saito, and H. Inokuchi, Chem. Lett. **1986**, 1037 (1986).
[35]H. Tajima, H. Kanbara, K. Yakushi, H. Kuroda, and G. Saito, Solid State Commun. **57**, 911 (1986) reported that $m_o(\|[\bar{1}10])/m_o(\perp[\bar{1}10])=3.5$ at 30 K.
[36]T. Mori, A. Kobayashi, Y. Sasaki, H. Kobayashi, G. Saito, and H. Inokuchi, Chem. Lett. **1984**, 957 (1984).
[37]M.-H. Whangbo, J. M. Williams, P. C. W. Leung, M. A. Beno, T. J. Emge, H. H. Wang, K. D. Carlson, and G. W. Crabtree, J. Am. Chem. Soc. **107**, 5815 (1985).
[38]J. Kübler, M. Weger, and C. B. Sommers, Solid State Commun. **62**, 801 (1987).
[39]K. Oshima, T. Mori, H. Inokuchi, H. Urayama, H. Yamochi, and G. Saito, Phys. Rev. B **38**, 938 (1988).
[40]K. Oshima (private communication).
[41]N. Toyota, T. Sasaki, K. Murata, Y. Honda, M. Tokumoto, H. Bando, N. Kinoshita, H. Anzai, T. Ishiguro, and Y. Muto, J. Phys. Soc. Jpn. **57**, 2616 (1988).
[42]K. Nozawa, T. Sugano, H. Urayama, H. Yamochi, G. Saito, and M. Kinoshita, Chem. Lett. **1988**, 617 (1988).
[43]R. P. Shibaeva, V. F. Kaminskii, and V. K. Bel'skii, Kristallografiya **29**, 1089 (1984) [Sov. Phys. Crystallogr. **29**, 638 (1984)].
[44]H. Kuroda, K. Yakushi, H. Tajima, and G. Saito, Mol. Cryst. Liq. Cryst. **125**, 135 (1985).
[45]H. Kuroda, K. Yakushi, H. Tajima, A. Ugawa, M. Tamura, Y. Okawa, A. Kobayashi, R. Kato, H. Kobayashi, and G. Saito, Synth. Metals **27**, A491 (1988).
[46]K. Bender, I. Henning, D. Schweitzer, K. Dietz, H. Endres, and H. J. Keller, Mol. Cryst. Liq. Cryst. **108**, 359 (1984).
[47]K. Yamaji, Solid State Commun. **61**, 413 (1987).
[48]W. L. McMillan, Phys. Rev. **167**, 331 (1968).
[49]T. Sugano, K. Terui, S. Mino, K. Nozawa, H. Urayama, H. Yamochi, G. Saito, and M. Kinoshita, Chem. Lett. **1988**, 1171 (1988).
[50]S. Katsumoto, S. Kobayashi, H. Urayama, H. Yamochi, and G. Saito, J. Phys. Soc. Jpn. **57**, 3672 (1988).
[51]The density of states $N(E_F)$ for the high-temperature (above 175 K) phase of β-(BEDT-TTF)$_2$I$_3$ was calculated by using the static paramagnetic susceptibility of 4.6×10^{-4} emu mol^{-1} at room temperature reported by B. Rothaemel, L. Forro, J. R. Cooper, J. S. Shilling, M. Weger, P. Bele, H. Brunner, D. Schweitzer, and H. J. Keller, Phys. Rev. B **34**, 704 (1986).
[52]V. N. Laukhin, E. E. Kostyuchenko, Yu. V. Sushko, I. F. Shchegolev, and E. B. Yagubskii, Pis'ma Zh. Eskp. Teor. Fiz. **41**, 68 (1985) [JETP Lett. **41**, 81 (1985)].
[53]K. Murata, M. Tokumoto, H. Anzai, H. Bando, G. Saito, K. Kajimura, and T. Ishiguro, J. Phys. Soc. Jpn. **54**, 1236 (1985).
[54]$N(E_F)$ used here was determined for the $T_c=8$ K (high-temperature) phase of β-(BEDT-TTF)$_2$I$_3$ and cannot be applied for the $T_c=1.5$ K phase.
[55]G. R. Stewart, J. O'Rourke, G. W. Crabtree, K. D. Carlson, H. H. Wang, J. M. Williams, F. Gross, and K. Andres, Phys. Rev. B **33**, 2046 (1986).
[56]M.-H. Whangbo, J. M. Williams, A. J. Schultz, T. J. Emge, and M. A. Beno, J. Am. Chem. Soc. **109**, 90 (1987).
[57]K. Oshima, H. Urayama, H. Yamochi, and G. Saito, Synth. Metals **27**, A473 (1988).
[58]G. C. Pimentel and A. L. McClellan, *The Hydrogen Bond* (Freeman, San Franciso, 1960), Chap. 3.
[59]T. J. Emge, H. H. Wang, U. Geiser, M. A. Beno, K. S. Webb, and J. M. Williams, J. Am. Chem. Soc. **108**, 3849 (1986).